3. Results

3.1 Characterization of LN cell populations during inflammation

In response to a paw inflammation lymphocytes homing towards the popliteal LN accumulate and proliferate which causes swelling of the tissue. The popliteal LN draining normal paw tissue accommodated about $2.8\times 10^5 \pm 1\times 10^5$ cells as determined using a cell counting chamber. Cell numbers changed significantly during the course of paw inflammation (Kruskal-Wallis Test, $P < 0.0001$). Fig. 3.1 A shows that in early inflammation (at 2 and 6 h) the number of LN cells were similar to controls (Dunn's Multiple Comparison Test, $P > 0.05$), but significantly increased at 24 h (30-fold, Dunn's Multiple Comparison Test, $P < 0.05$) and at 96 h (170-fold, Dunn's Multiple Comparison Test, $P < 0.001$) after CFA-inoculation. To assess changes of the cell subsets LN cells were analyzed using flow cytometry (Fig. 3.1 B - F). Cells were stained with monoclonal antibodies to identify B-cells (anti-IgG Kappa-FITC), all T-cells (anti-CD3-PE), cytotoxic T-cells (anti-CD8-FITC) or T helper cells and monocytes/macrophages (anti-CD4-FITC). Cells were double-stained by anti-CD3 and anti-CD4 to identify monocytes as $CD3^-/CD4^+$ cells.

The proportion of B-cells significantly increased at 96 h of CFA inflammation (One-way ANOVA, $P < 0.005$; Dunnett's Multiple Comparison Test, $P < 0.01$, Fig. 3.1 B). The proportion of $CD3^+$ T-cells decreased significantly at 96 h after CFA-injections (One-way ANOVA, $P < 0.005$; Dunnett's Multiple Comparison Test, $P < 0.05$; Fig. 3.1 C). These changes resulted in significantly decreased T-to-B-cell ratios (4:1 in controls vs. 1:1 at 96 h, One-Way ANOVA and Dunnett's Multiple Comparison Test; $P < 0.05$). The proportion of $CD4^+$ cells did not change significantly between control and inflammatory conditions (One-way ANOVA, $P > 0.05$, Fig. 3.1 D). The proportion of $CD8^+$ T-cells significantly increased at 48 h after CFA-injections (One-way ANOVA, $P < 0.05$; Dunnett's Multiple Comparison Test, $P < 0.05$; Fig. 3.1 E). The abundance of $CD4^+$ cells exceeded that of $CD8^+$ cells in controls (Fig. 3.1 F). The $CD4^+/CD8^+$-cell ratios were significantly decreased at all time points analyzed during inflammation (One-Way ANOVA, $P<0.0001$; Dunnett's Multiple Comparison Test; 0 vs 24: $P < 0.01$, 0 vs 48: $P < 0.01$, 0 vs 96: $P < 0.01$, Fig. 3.1 F). The proportion of monocytes was 5 - 10% under both control and inflammatory conditions and displayed no statistically significant changes (One-way ANOVA, $P > 0.05$, Fig. 3.1 D).

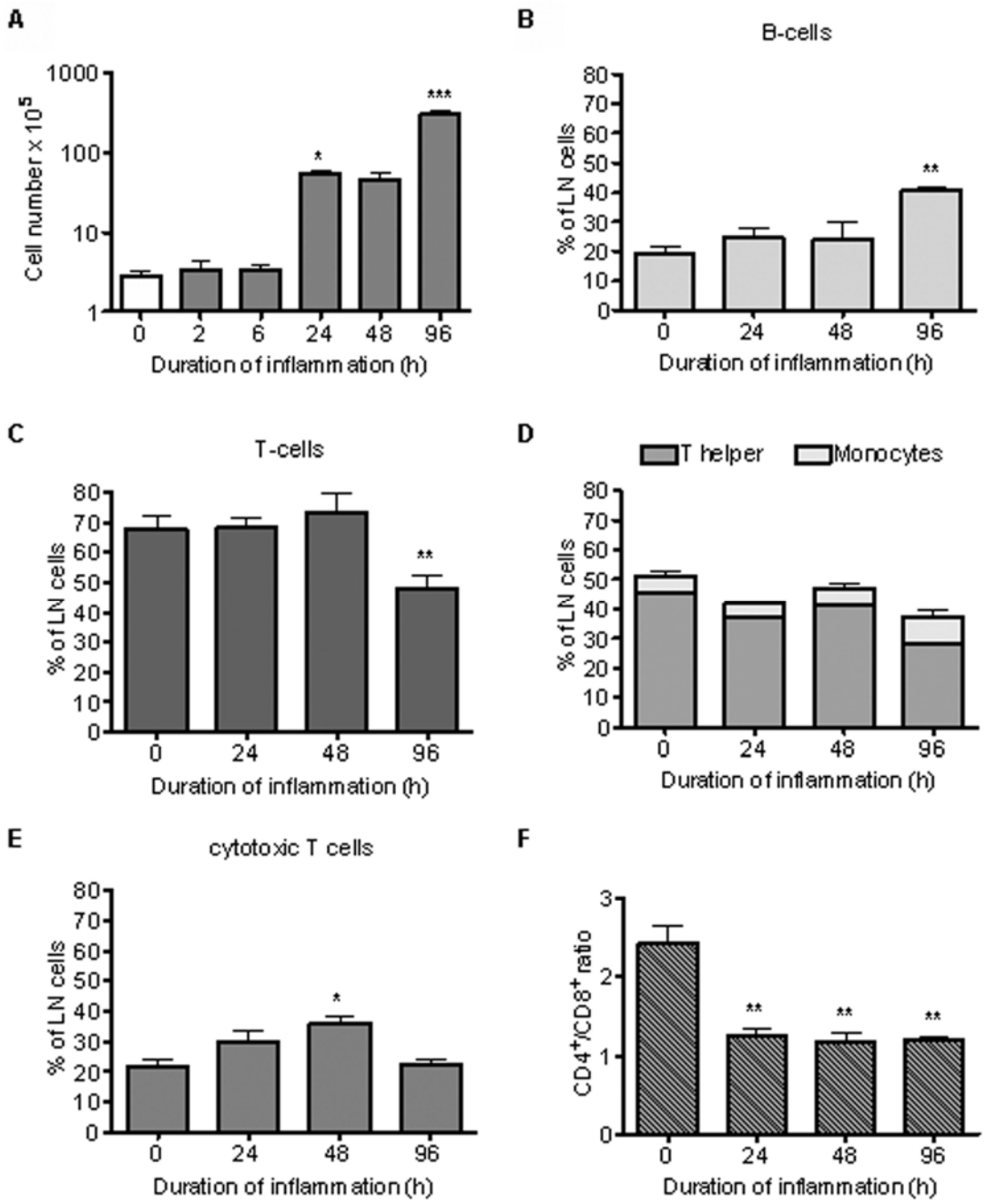

Fig. 3.1 Distribution of LN cell subsets during the development of paw inflammation. Popliteal LN were dissected from 3 - 4 animals each at 0 - 96 h after CFA-induced inflammation. **A.** Cell numbers of LN draining normal and inflamed paw tissue. Cell numbers are given along the y-axis (log10 scaling). Data were analyzed with Kruskal-Wallis and Dunn's Multiple Comparison Test. **B – F.** Flow cytometry analysis of LN cell subsets during inflammation. Cells were stained with monoclonal antibodies for **B**) B-cells (IgG Kappa-FITC), **C**) T-cells (CD3-PE), **D**) T helper cells and monocytes/macrophages (CD4-FITC) or **E**) cytotoxic T-cells (CD8-FITC). 10,000 events per LN were analyzed. Cell numbers are given as% in means ± SD of total LN cells along the y-axis in **A - D**. **F**) $CD4^+/CD8^+$ ratios of T-cells in the course of inflammation. Data represent means ± SD of 3 samples per treatment group. All data were analyzed with One-Way ANOVA and Dunnett's Multiple Comparison Test. *P < 0.05, **P < 0.01, ***P < 0.001.

3.2 POMC mRNA expression in lymphocytes

3.2.1 RT-PCR and primer conditions

Since previous attempts to analyze POMC transcripts in lymphocytes using RT-PCR were unsuccessful (Galin et al. 1991; van Woudenberg et al. 1993), the suitable PCR conditions and primer pairs needed to be established. An initial denaturation time of 5 min and a final elongation time 10 min were chosen. During cycling, the denaturating step was extended from 30 to 45 sec. Several POMC primer pairs (see Table 2.3) were tested to generate amplicons spanning different parts of POMC mRNA under these conditions. All transcripts were successfully amplified at different annealing temperatures (AT) between 55 - 68°C from pituitary, which served as a positive control.

Two primer pairs were tested to amplify exon 3 fragments of POMC mRNA from LN. Both of them generated amplicons of the appropriate size using AT ranging from 62°C to 67°C (Ex3A and Ex3B, Fig. 3.2). Amplification of POMC exon 2 transcripts from LN-derived cDNAs revealed pituitary-like PCR products using an AT of 61°C (Ex2, Fig. 3.2).

Among the primer pairs tested to amplify POMC exon 2-3 transcripts, 3 out of 19 primer pairs generated pituitary-like transcripts from LN-derived cDNAs, when the assays were run with distinct AT of 63.2°C for Ex2-3E, 66°C for Ex2-3F, and 59°C for Ex2-3G (Fig. 3.2).

For the amplification of POMC exon 1-2 spanning transcripts 2 primer pairs were tested and one of them revealed amplicons from LN samples identical in size to the pituitary PCR product, while the other revealed no product. The detectable POMC exon 1-2 mRNA fragment was amplified from LN samples using an AT of 55°C (Ex1-2B, Fig. 3.2).

Fifteen primer pairs were tested to generate POMC transcripts spanning all 3 exons. Two primer pairs revealed amplicons of the appropriate sizes from LN samples at an AT of 61°C (Ex1-3F, Fig. 3.2) and 63.2°C (Ex1-3O, Fig. 3.2).

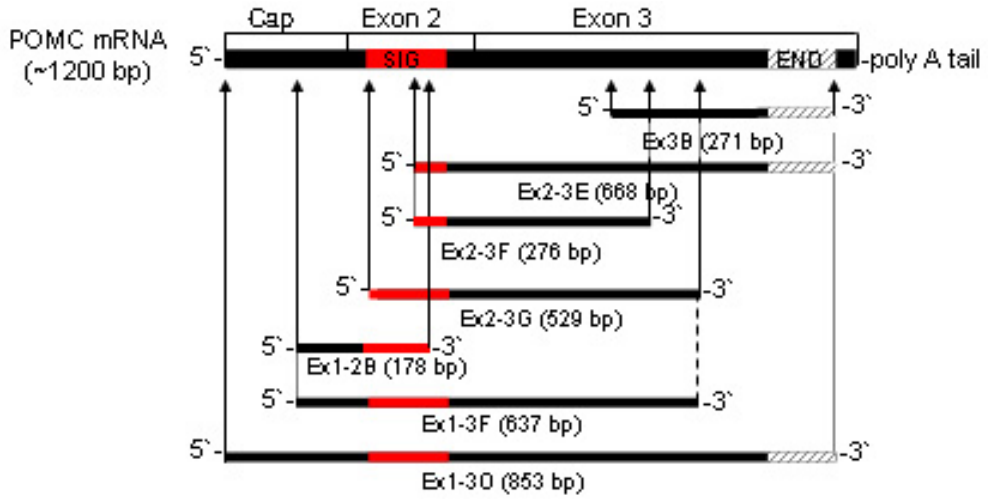

Fig. 3.2 Schematic overview of primer pairs revealing POMC mRNA amplicons from LN. The signaling sequence (SIG) is red, END is hatched. The primer positions are indicated by arrows. Details on the different primer pairs are listed in the methods section.

3.2.2 Expression of POMC mRNA including the signal sequence in lymphocytes

To analyze, whether lymphocytes from control and CFA-treated animals express different POMC transcripts, LN-derived cDNAs were amplified using RT-PCR applying the conditions described above (see 3.2.1). First, RNA qualities were analyzed comparing the intensity of 28S and 18S ribosomal RNA bands to rule out RNA degradation during storage of frozen tissue. All RNAs were intact and showed 28S ribosomal RNA bands with intensity twice that of the 18S RNA ribosomal band (Fig. 3.3).

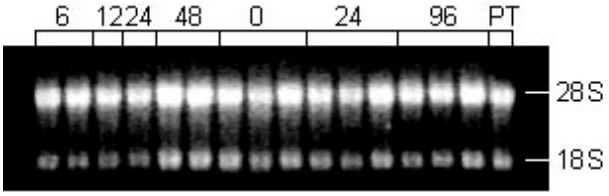

Fig. 3.3 Formaldehyde-agarose gel electrophoresis of total RNA from LN and pituitary tissues. Total RNA (1 µg) from frozen pituitary (PT) and from LN of animals with 0 - 96 h CFA-inflamed hindpaws was separated electrophoretically. Ribosomal bands (28S and 18S) are shown.

POMC exon 2-3 spanning amplicons similar to those derived from pituitary including the entire signal sequence were found in LN from untreated animals and in popliteal LN at 6, 12, 24, and 48 h after ipsilateral CFA-induced paw inflammation (Fig. 3.4 B). Thus, signal sequence containing POMC mRNA spanning exon 2-3 was detectable in all inflamed LN. Pituitary-like POMC exon 1-3 spanning amplicons of 637 and 853 bp were found occasionally in draining LN at 2, 6, 12, 24 and 96 h after CFA-inoculation of the paw but not in LN from untreated animals (Fig. 3.4 C and D).

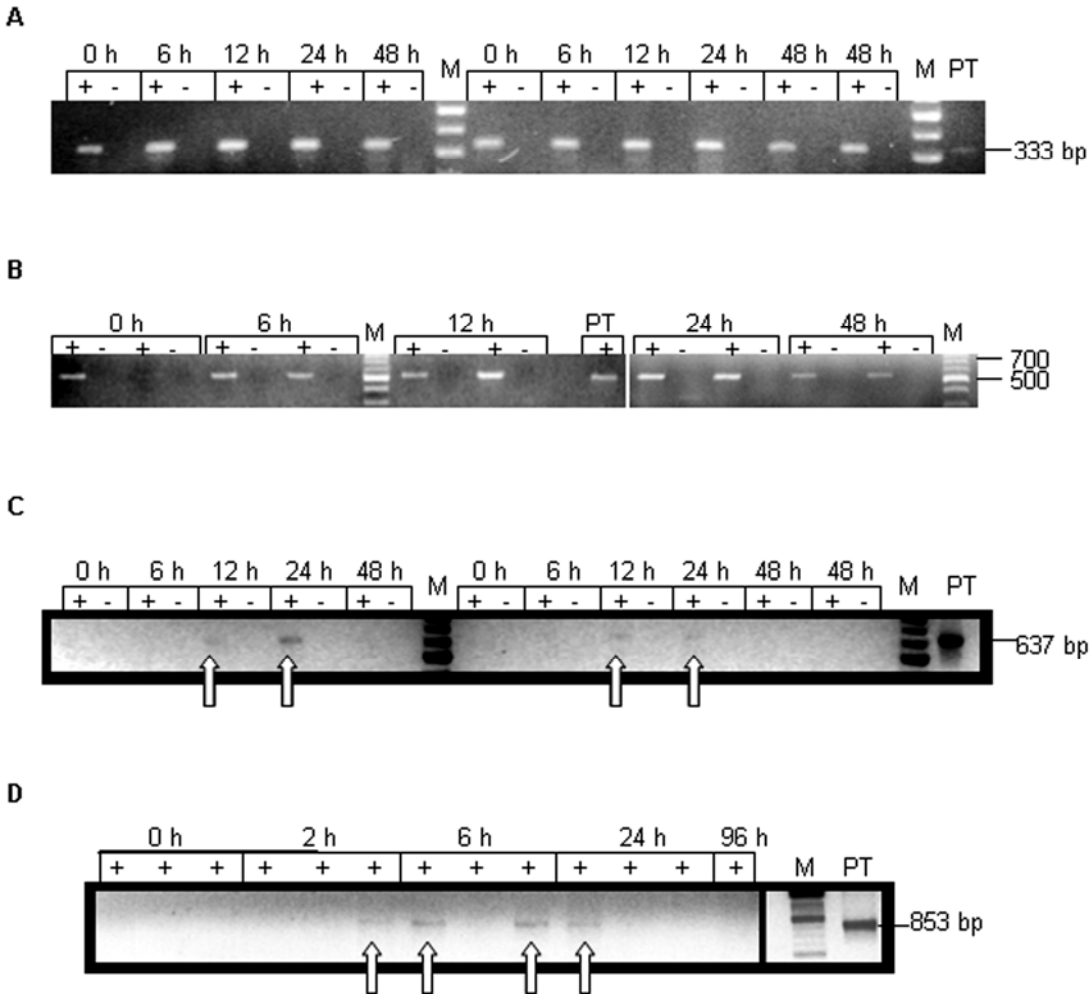

Fig. 3.4 Pituitary-like POMC mRNA including the signal sequence is expressed in LN tissue. Total RNA was isolated from popliteal LNs draining CFA-inflamed paw tissue for 0 - 96 h and from pituitary. RT-PCR products were electrophoretically separated and visualized under UV-light. **A.** RpL19 transcript of 333 bp. **B.** POMC Ex2-3G (529 bp). **C.** POMC Ex1-3F (637 bp). **D.** POMC Ex1-3O (853 bp). Arrows point towards weak product bands. Adjacent lanes labeled with (+) and (–) represent reverse transcribed and genuine RNA of the same sample, respectively. M = 100 bp standard DNA marker; PT = pituitary

3.2.3 Expression of POMC mRNA in cell subsets of LN

To analyze the expression of POMC mRNA in LN cell subsets, cells were separated into T- and B-cells using magnetic beads. The efficiency of such magnetic separation was verified by flow cytometry. Fig. 3.5 gives an example for the purity of cell fractions separated with PanTcell microbeads. About 50% T-, 40% B-cells, and 5 - 10% non-T-non-B-cells were present in LN draining CFA-inflamed paw tissue (Fig. 3.5 A). Following magnetic cell separation, the T-cell enriched fraction ($CD3^+$) contained 90% T-cells, 6% B-cells, and showed a proportion of about 4% non-T-non-B-cells (Fig. 3.5 B). The T-cell depleted fraction ($CD3^-$) showed 3% remaining T-cells, while B-cells were enriched to 72% (Fig. 3.5 C). The non-T-non-B-cells made up to 25% in the T-cell

depleted fraction (Fig. 3.5 C). The purity of separated control LN fractions was similar (data not shown). POMC exon 2-3 spanning transcripts were detected in $CD3^+$ and $CD3^-$ cell fractions from LN draining normal and inflamed paw tissue (Fig. 3.5 D), but were detectable in separated LN cells from normal animals only by semi-nested RT-PCR.

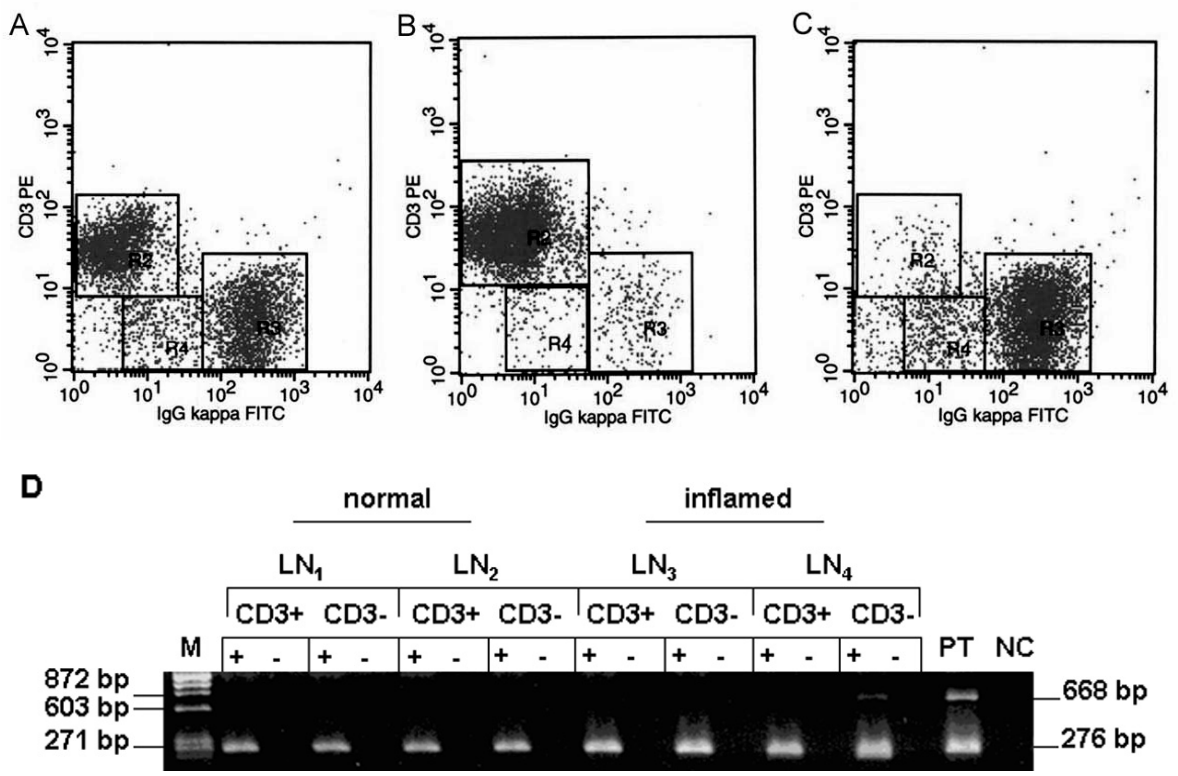

Fig. 3.5 Identification of exon 2-3 spanning POMC mRNA transcripts in T- and B-cell-enriched LN cell fractions. **A - C**. Popliteal LN were dissected at 96 h after induction of inflammation and cells were separated using PanTCell microbeads. Proportions of T-cells ($CD3^+$, R2), B-cells (IgG $kappa^+$, R3), and non-T-non-B-cells (R4) were determined using flow cytometry before separation (**A**), in $CD3^+$-fractions (**B**), and in $CD3^-$-fractions (**C**). Dot blots show log10 fluorescence along both x- and y-axis. **D.** Agarose gel electrophoresis of exon 2-3 spanning POMC mRNA transcripts in separated LN cells. Total RNA was isolated from T-cell positive ($CD3^+$) and T-cell negative ($CD3^-$) LN cell fractions from two animals without inflammation ($LN_{1, 2}$) and from two animals at 96 h after CFA-inoculation ($LN_{3, 4}$). Using semi-nested RT-PCR, exon 2-3 spanning POMC fragments (276 bp) were re-amplified using RT-PCR. M = 72 - 1353 bp DNA ladder; NC = water control; PT = pituitary; + = reverse transcribed RNA samples, - = genuine RNA samples

POMC transcripts spanning exon 3, exons 2-3, exons 1-2, and exons 1-3 mRNA were amplified using RT-PCR from identical cDNA samples and the electrophoretical separation of $CD3^+$- and $CD3^-$-derived RT-PCR products is shown in Fig. 3.6. The cDNA-quality of each sample was verified by the amplification of exon 2-5 spanning rpL19 transcripts. RpL19 mRNA was detected in all samples (data not shown). POMC exon 3 fragments were detected in all $CD3^+$ and $CD3^-$ samples (Fig. 3.6 A); RT^--controls showed

no contamination but in one $CD3^+$ LN fraction (RT^-control of $CD3^+_1$ in lane 3, Fig. 3.6 A). POMC exon 1-2 spanning amplicons of 178 bp were detectable in all $CD3^-$ samples but not in $CD3^+$ samples (Fig. 3.6 B). Pituitary-like POMC exon 2-3 spanning transcripts of 668 and 529 bp length were detectable in both $CD3^+$ and $CD3^-$ samples (Fig. 3.6 C and D, respectively). Amplification of POMC exon 1-3 spanning fragments revealed no detectable PCR product bands in any fraction (data not shown). Sequences of LN- and pituitary-derived POMC fragments spanning the second and third exon were 97% identical to each other. Alignments of original sequencing data with NCBI Blast POMC data strings are given in Appendix B. The shorter exon 2-3 POMC mRNA fragment of 529 bp, contained the complete signal sequence and parts of exon 3 including ACTH but not the END sequence (Appendix B, Fig. A.1). Larger POMC exon 2-3 transcript of 668 bp contained the END sequence and 10 bp of the signal sequence (Appendix B, Fig. A.2). In both cases, the 3% differences in sequences between pituitary and lymphocytic POMC sequences diminished to < 0.5% after detailed analysis of the chromatograms and correction of gaps and unidentified nucleotides.

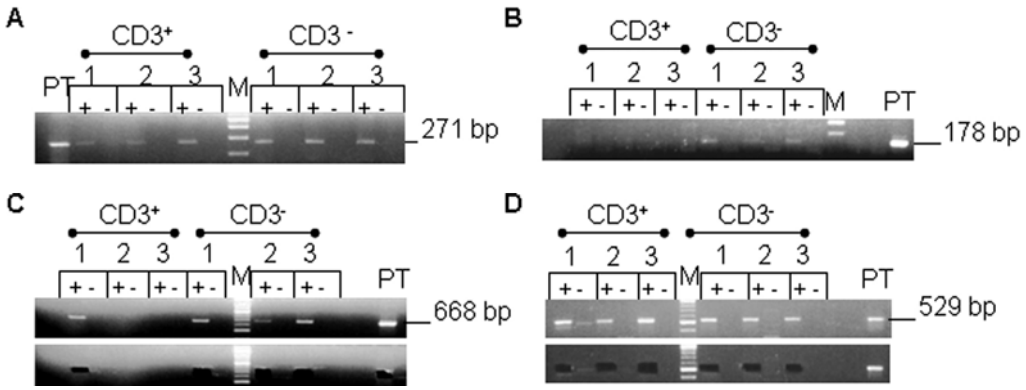

Fig. 3.6 Comparison of different POMC mRNA fragments in separated LN cells. Oligo dT-cDNAs from $CD3^+$ and $CD3^-$ LN cells of three animals with 96 h CFA-inflammation were amplified using RT-PCR. **A - D.** Electrophoretically separated PCR products. **A.** POMC Ex3B (271 bp), **B.** POMC Ex1-2B (178 bp), **C.** POMC Ex2-3E (668 bp), and **D.** POMC Ex2-3G (529 bp). Lower panels of C and D demonstrate cut outs of product bands analyzed by sequencing. P = pituitary, M = 100 nt DNA ladder, + = reverse transcribed RNA samples, - = genuine RNA samples

To investigate the 5`-ends of POMC amplicons and to clarify whether the POMC exon 3 expression is related to alternative transcription initiation sites within exon 3 or its 5`-end flanking region, separated LN cells were analyzed using nested RACE-PCR. Only one of the three nested primer pairs tested occasionally revealed PCR products of the expected size in LN (5´-N-RACE 3, Table 3.2). Fig. 3.7 A shows this 369 bp fragment in $CD3^+$ LN cells and in pituitary. For an example of the sequence alignment of these products see Appendix C (Fig. A.3). The $CD3^+$ cell-derived sequence contained the same part of exon 1 forming the 5-end cap region as found in the pituitary sequence. Both sequences represented a shorter splicing variant of POMC that characteristically lacks 30 bp of the 5`-end exon 2 region. The predominant amplicons generated from separated LN cells were 200 - 300 bp smaller than in pituitary (Fig. 3.7 B). Sequencing of these short N-RACE-PCR products provided no exon 1- or exon 2-like regions but contained exon 3 and parts of intron B (see Appendix C, Fig. A.4). The sequence analysis of eight different N-RACE-PCR products revealed variable parts of intron B, causing the different product sizes for example seen in Fig. 3.7 B.

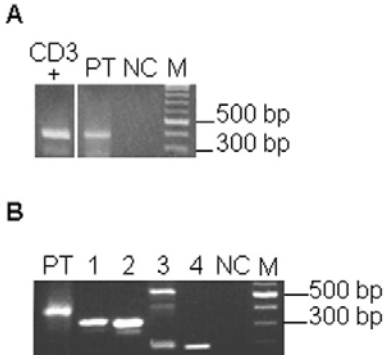

Fig. 3.7 RACE-PCR provides full-length and truncated POMC mRNA variants in separated LN cells. Total RNA was isolated from LN cell fractions and from pituitary (PT). RACE-PCR products (5´-RACE 3) were re-amplified and the nested PCR products (5´-N-RACE 3) were electrophoretically separated. The expected product size was ~369 bp. **A.** Full-length POMC transcripts in PT and $CD3^+$ LN cells. **B.** Truncated POMC transcripts. 1 = $CD3^+$ LN_1, 2 = $CD3^+$ LN_2, 3 = $CD3^-$ LN_1, 4 = $CD3^-$ LN_2, M = 100 bp DNA marker, NC = negative water control

3.2.4 Quantification of POMC mRNA

3.2.4.1 Upregulation of POMC exon 2-3 versus POMC exon 3 mRNA

For quantitative analysis of POMC expression levels in LN, the qRT-PCR was calibrated with DNA-standards specifically generated for the transcripts Ex3B and Ex2-3F (see Fig. 3.2) and for the housekeeping gene rpL19. These standards contained about 2 - 3× 10^{10} copies/µl each and were tested to determine the detection range of the qRT-PCR as well as the melting points of the PCR products. Standard dilution from 10^{10} to 10^{3} copies revealed detectable amplicons for all three transcripts. Samples that contained < 10^{3} copies showed low signal-to-noise ratios but still provided detectable amplicons for all three transcripts. Fig. 3.8 shows examples of the curves obtained after amplification of 10^{7} to 10^{4} copies each. All curves showed similar slope parameters and the PCR efficiencies of all three transcripts ranged from 1.75 to 1.9. RpL19-specific products melted between 88 - 90°C, while POMC exon 3 and POMC exon 2-3 products melted between 90 - 92°C (data not shown). Therefore, the temperatures chosen for the measurement of transcript-specific fluorescence during cycling were 89°C for rpL19 and 91°C for POMC transcripts.

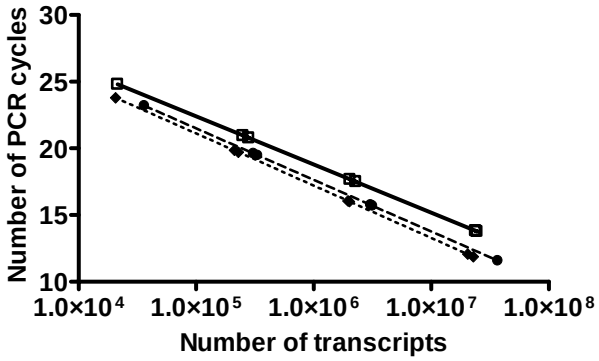

Fig. 3.8 DNA-standard curves for rpL19 and POMC quantification. DNA standards for rpL19 (□), Ex3B (♦), and Ex2-3F (●) were generated from pituitary cDNA. Standard curves had the following parameters: $y_{POMC\ exon\ 3}$ = -1.7013Ln(x) + 40.706, r2 = 1; y_{rpL19} = -1.5668Ln(x) + 40.441, r2 = 1; $y_{POMC\ exon\ 2\text{-}3}$ = -1,6756Ln(x) + 40,778, r2 = 1. PCR efficiencies were 1.893 for rpL19, 1.800 for Ex3B and 1.816 for Ex2-3G.

To investigate expression levels of truncated or signal sequence containing POMC transcripts, the amounts of Ex3B and Ex2-3F were analyzed relative to the expression of rpL19 at different time intervals during CFA-induced paw inflammation. The amplification of the POMC templates from LN yielded low signal-to-noise ratios. LN

contained 1000 - 8000 POMC exon 3 copies and 100 - 500 POMC exon 2-3 copies per μg total RNA. In pituitary 2 - 8× 10^8 copies of POMC exon 3 and 2-3 transcripts were detected per μg total RNA. RpL19 transcripts reached amounts of 1× 10^6 to 1× 10^7 copies per μg total RNA in LN and 3 - 9× 10^7 copies per μg total RNA in pituitary. The average Ex3B/rpL19 ratio was 10^3 fold higher in pituitary than in LN (compare Fig. 3.9 B and A, respectively). The Ex2-3F/rpL19 ratio was 10^4 fold higher in pituitary than in LN (compare Fig. 3.9 D and C, respectively). In LN the ratio of Ex3B/rpL19 was 10 times higher than the ratio of Ex2-3F/rpL19 (compare Fig. 3.9 A and C). In the course of paw inflammation ratios of Ex3B/rpL19 did not change in LN or pituitary (One-Way ANOVA: $P_{LN} > 0.05$ and $P_{PG} > 0.05$, Fig. 3.9 A and B). The Ex2-3F/rpL19 ratio significantly increased after CFA-treatment in LN (One-Way ANOVA, $P < 0.0005$, Fig. 3.9 C) but not in pituitary (One-Way ANOVA, $P > 0.05$, Fig. 3.9 D). At 2 h of paw inflammation Ex2-3F/rpL19 ratios were 6-fold higher than in controls (Dunnett's Multiple Comparison Test, $P < 0.01$, Fig. 3.9 C).

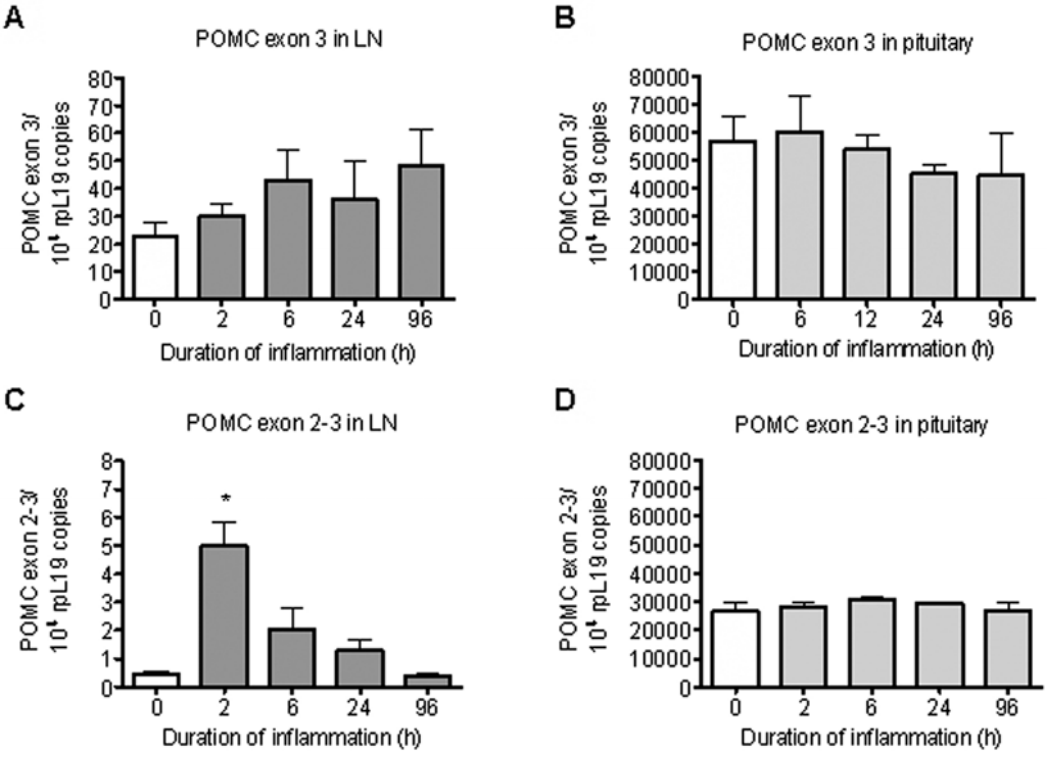

Fig. 3.9 Ratios of POMC exon 2-3/rpL19 and of POMC exon 3/rpL19 during paw inflammation. Amounts of POMC and rpL19 transcripts were determined in LN and pituitary at 0 - 96 h of inflammation using single-round QRT-PCR. Samples were measured in triplicates. **A.** Ratios of Ex3B/rpL19 copies in LN, n = 3. **B.** Ratios of Ex3B/rpL19 in pituitary, n = 2. **C.** Ratios of Ex2-3F/rpL19 in LN, n = 3. **D.** Ratios of Ex2-3F/rpL19 in pituitary, n = 2. All values represent means ± SD. Data were analyzed using One-Way ANOVA and Dunnett's Multiple Comparison Test, **P < 0.01.

3.2.4.2 Semi-nested qRT-PCR enhances sensitivity for POMC exon 2-3 detection

To improve the low signal-to-noise ratios nested qRT-PCR was used instead of single-round qRT-PCR. Two larger POMC exon 2-3 spanning fragments (Ex2-3E and Ex2-3G, see Fig. 3.2 and Fig. 3.10 A) were pre-amplified and these PCR products were subsequently re-amplified using a primer pair to obtain the smaller POMC fragment Ex2-3F (see Fig. 3.2 and Fig. 3.10 A). These primers were used both as a nested and a semi-nested primer pair (Fig. 3.10 A). In both cases, PCR products of the expected size (276 bp) were generated (Fig. 3.10 B and C). When used as a nested primer pair, larger secondary PCR products were also detected (Fig. 3.10 B). When used as semi-nested primer pair, the re-amplification revealed a single PCR product (Fig. 3.10 C).

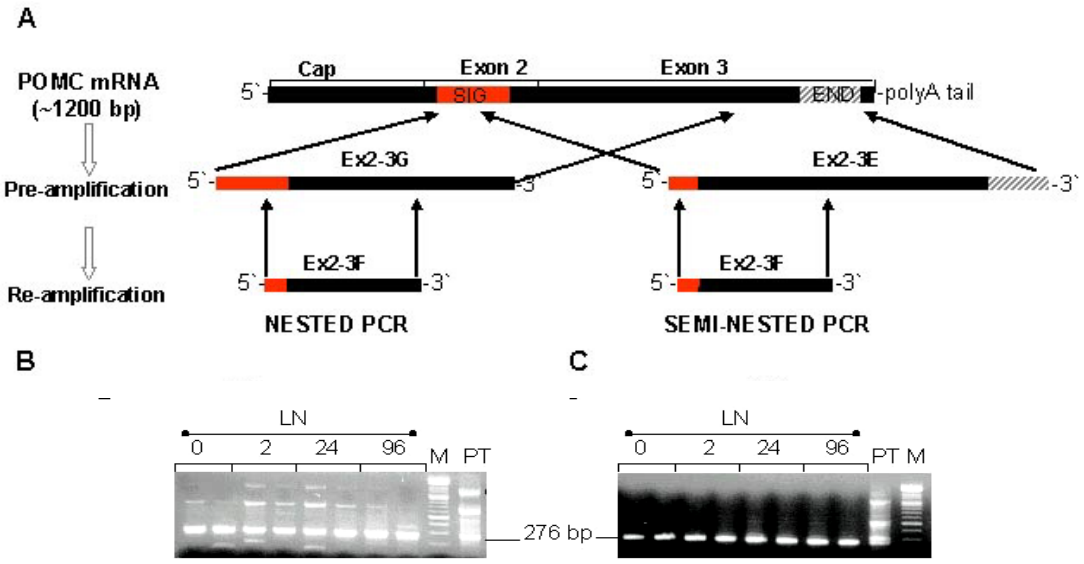

Fig. 3.10 Exon 2-3 POMC transcripts in popliteal LN generated with nested and semi-nested qRT-PCR. Popliteal LN (n = 2) were analyzed at 0 - 96 h of paw inflammation. **A.** Scheme of nested/semi-nested qRT-PCR. **B.** Nested PCR products after pre-amplification of Ex2-3G (529 bp). **C.** Semi-nested PCR products after pre-amplification of Ex2-3E (668 bp). Nested/semi-nested PCR products (Ex2-3F, 276 bp) were electrophoretically separated and visualized under UV-light. PT = pituitary; M = 100 bp standard DNA marker

The semi-nested qRT-PCR strategy revealed that the relative expression of POMC exon 2-3 spanning transcripts in LN was significantly upregulated at 2 and 6 h of paw inflammation (One-Way ANOVA, $P < 0.005$; Dunnett's Multiple Comparison Test, 0 vs. 2 h: $P < 0.01$; 0 vs. 6 h: $P < 0.05$, Fig. 3.11 A), and thus reproduced the results obtained in single-round qRT-PCR assays. The relative POMC expression was not increased at later time points analyzed (Dunnett's Multiple Comparison Test, 0 vs. 24 h: $P > 0.05$; 0 vs. 96 h: $P > 0.05$, Fig. 3.11 A). The semi-nested qRT-PCR products had a

specific melting peak at 93°C (Fig. 3.11 B) and sequences were identical to that of pituitary amplicons (data not shown).

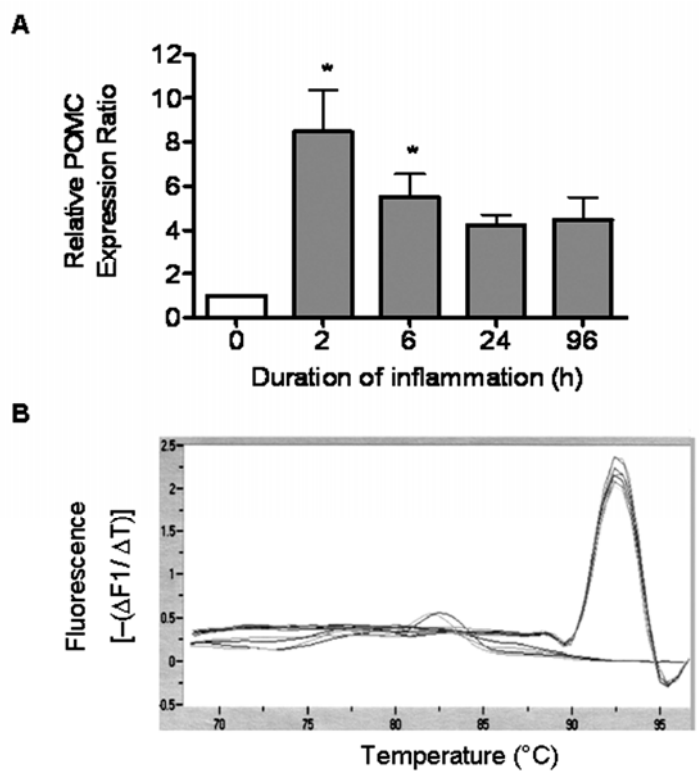

Fig. 3.11 Relative expression of exon 2-3 POMC mRNA in LN during the development of paw inflammation. Total RNA was isolated from LN at 0 - 96 h after CFA-inoculation. POMC exon 2-3 spanning transcripts (Ex2-3F) were quantified using semi-nested qRT-PCR. Samples were measured in duplicate. **A.** Data represent mean POMC expression ratios relative to noninflamed controls ± SD of six LN per group. Statistical analysis was done with One Way ANOVA, $P < 0.05$ was defined as significant. **B.** Melting curve analysis of semi-nested qRT-PCR products.

3.3 Expression profile of prohormone convertases in lymphocyte subsets

Proteolytic cleavage of the POMC prohormone requires two prohormone convertases PC1/3 and PC2, and the chaperone 7B2 (Benjannet et al. 1991; Benjannet et al. 1995). To investigate which enzymes are expressed in T- or B-cell-enriched fractions from control LN and after induction of a unilateral CFA-inflammation the mRNA of all three enzymes was amplified using RT-PCR. Pituitary and macrophages served as positive controls and both tissues expressed all three genes (Fig. 3.12). PC1/3 expression was undetectable in $CD3^+$ and $CD3^-$ cell fractions from control LN and contralateral LN at 24 h after CFA-inoculation (Fig. 3.12). In contrast, the $CD3^-$ fraction from ipsilateral LN at 96 h after CFA-inoculation expressed PC1/3 (Fig. 3.12). PC2 expression was detected in all $CD3^+$ cell fractions, while $CD3^-$ cells expressed this enzyme only at 96 h of inflammation time (Fig. 3.12). 7B2 was expressed in all samples analyzed (Fig. 3.12). Similar results as presented in Fig. 3.12 were obtained in two other experiments.

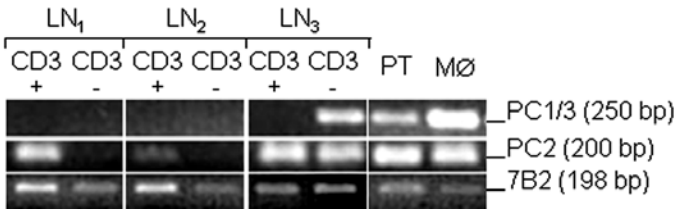

Fig. 3.12 Expression of PC1/3 and PC2 and of 7B2 mRNAs in LN cell subsets. Total RNA was isolated from $CD3^+$ and $CD3^-$ popliteal LN cell fractions, pituitary (PT), and macrophages (M∅). PC1/3, PC2 and 7B2 mRNA transcripts were analyzed using RT-PCR. PCR products were electrophoretically separated and visualized under UV-light. LN_1 = control LN; LN_2 = contralateral LN at 24 h after CFA-inoculation; LN_3 = ipsilateral LN at 96 h after CFA-inoculation

3.4 Identification of END-containing lymph node cells

3.4.1 Characterization of the polyclonal END antibody

To characterize the specificity of the polyclonal END antibody from Peninsula Laboratories, which was used for immunohistchemistry and RIA, pituitary lysates from wild type and END$^{-/-}$ mice (provided by M. Low, Oregon Health Sciences University, Portland, USA) were analyzed using RIA. In these END$^{-/-}$ mice the codon for the N-terminal tyrosine of END was changed into a premature translational stop codon by site-directed mutagenesis. This mutation leads to the selective ablation of the C-terminal sequence encoding END, leaving the production of other POMC derived peptides intact (Rubinstein et al. 1996). In protein dilution of 1:100 and 1:1000 wild type mice contained about 300 and 30 pg ir-END/tube, respectively (Fig. 3.13 A), while the ir-END of END$^{-/-}$ pituitaries was always below detection limit (< 8 pg/tube, Fig. 3.13 A). Tail biopsies were analyzed using RT-PCR. As shown in Fig. 3.13 B the mutant but not the wild type POMC allele was present in END$^{-/-}$ animals and wild types showed no mutant allele.

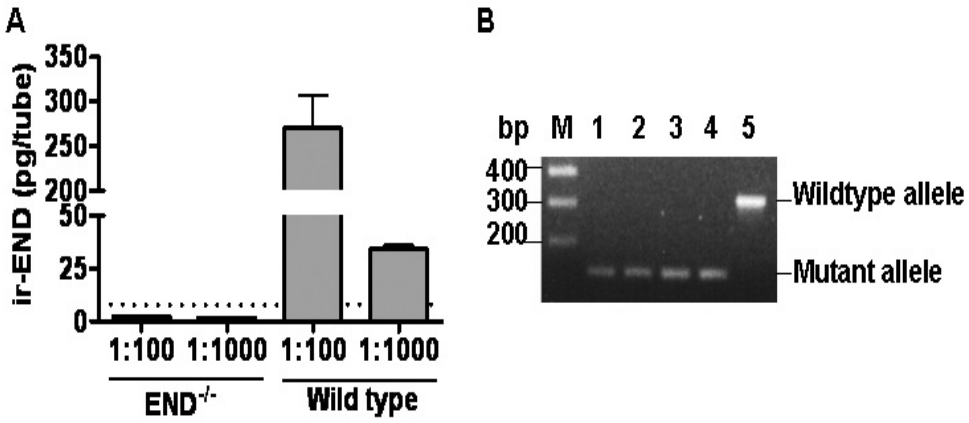

Fig. 3.13 Quantification of ir-END in wild type and END$^{-/-}$ mouse pituitaries. **A.** Pituitary lysates of wild type and END$^{-/-}$ mice were analyzed using RIA to test the END antibody specificity. Values represent the mean ir-END ± SD from n = 7 animals per group as measured in 100 µl of diluted pituitary lysates (1:100 and 1:1000). The detection limit was < 8 pg/tube (dotted line). In END$^{-/-}$ mice ir-END was not detectable. **B.** Genotyping of wild type and END$^{-/-}$ mice. The DNA of five animals was analyzed using RT-PCR. The wild type and mutated allele could be distinguished by their differences in size (316 bp in wild type and 159 bp in END$^{-/-}$ mice). *Lanes 1-4*: END$^{-/-}$ animals, *lane 5*: wild type.

3.4.2 Co-localization of ir-POMC and ir-END in lymphocytes

LN tissues draining normal (Fig. 3.14 A - D) and inflamed (Fig. 3.14 E - H) paws were analyzed using immunofluorescence to identify co-localization of ir-POMC and ir-END. Several cells of the paracortical and medullar region in control and inflamed LN were POMC-positive (Fig. 3.14 B and F) and END-positive (Fig. 3.14 A and E). Similarly, the cortical region showed staining with both antibodies (data not shown). Ir-POMC and ir-END were co-localized in the majority of positive cells of controls (Fig. 3.14 C) and of 24 h inflamed LN (Fig. 3.14 G). Under both conditions only few cells expressed ir-POMC alone (Fig. 3.14 C and G). Ir-POMC- and ir-END-positive cells made up about 10 - 20% of the total cell number (Fig. 3.14 D and H).

At 96 h of paw inflammation, ir-END was identified in several LN lymphocytes and in fewer monocytes/macrophages (Fig. 3.15, upper panel). Ir-POMC was detected in both cell types (Fig. 3.15, lower panel) using a polyclonal POMC antibody that binds to the N-terminal POMC region. Lymphocytes were morphologically identified by large, regularly shaped nuclei surrounded by small amounts of cytoplasm (Fig. 3.15, upper and lower panel). Macrophages showed irregular-shaped nuclei surrounded by cytoplasm (Fig. 3.15, upper and lower panel). POMC and END stains were stronger in monocytes/macrophages compared to lymphocytes.

Fig. 3.14 (next page) Co-localization of ir-POMC and ir-END in control and inflamed LN. Sections of control (**A - D**) and inflamed LN (**E – H**) were analyzed using double immunofluorescence of ir-POMC (**A, E**) and ir-END (**B, F**). Note that the majority of ir-POMC cells (green) contain ir-END (red) as indicated by yellow color in **C** and **G** (double arrows). Few cells show only ir-POMC (single arrows in **C** and **G**). **D + H.** Double immunofluorescence of POMC and END and counterstaining of cell nuclei with DAPI (blue). Note that not all LN-cells express POMC and/or END. Double arrows point towards POMC/END-negative cells with a blue nucleus but without red, green or yellow fluorescence. **I.** Control staining without primary antibodies counterstained with DAPI. Bar = 10 µm.

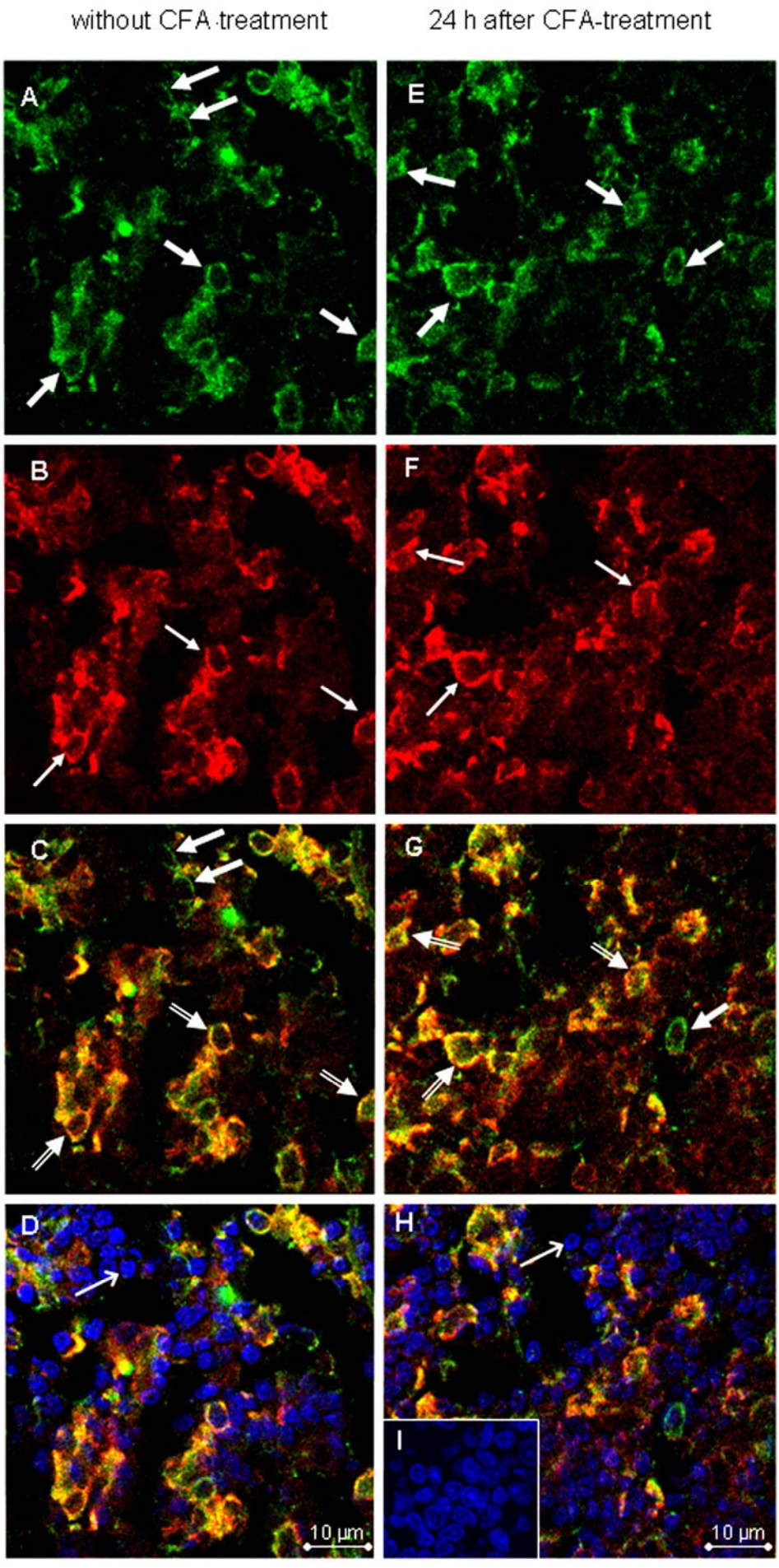
without CFA-treatment
24 h after CFA-treatment
A
E
B
F
C
G
D
H
I
10 µm
10 µm

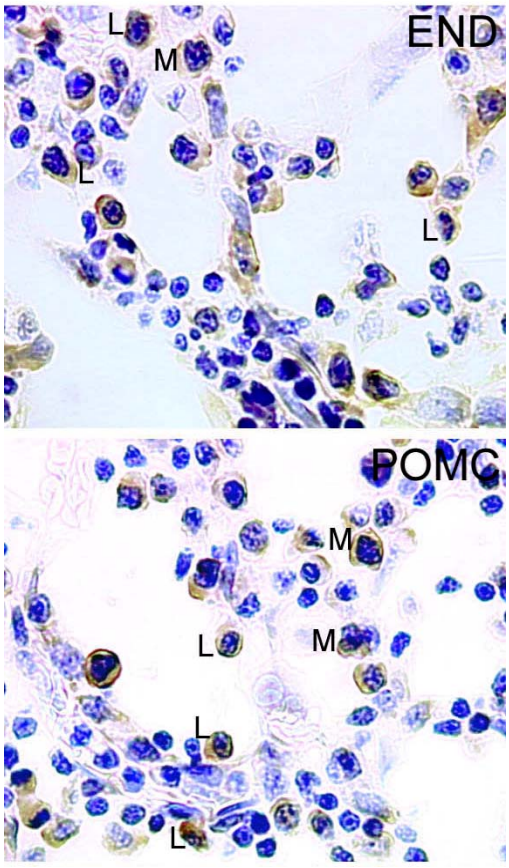

Fig. 3.15 Morphological identification of POMC- and END-expressing LN cells draining inflamed paw tissue. Ir-END (**upper panel**) and ir-POMC (**lower panel**) detected by brown extranuclear staining in macrophages/monocytes (M) and lymphocytes (L) in inflamed LN sections (96 h CFA). The nuclei counterstained with thionin appear blue.

3.4.3 Magnitude of opioid peptide-expressing cell subsets in inflamed LN

LN-derived cells were stained intracellulary using a monoclonal mouse pan-opioid primary antibody (3E7) and a PE-labeled rat anti-mouse secondary antibody (RAM PE) for flow cytometry analysis. Specificity of staining was verified by using an isotype matched control (IgG 2a), non-specific binding was 2% (Fig. 3.16 B). The percentage of $3E7^+$ cells was 9.5 ± 2% in regional LN draining 96 h CFA-inflamed hindpaws (n = 5) (Unpaired t test, $P < 0.005$). An example is given in Fig. 3.16 C.

To investigate the distribution of endogenous opioids within LN cell subsets at 96 h after CFA-inoculation of the paw (n = 5), cells were double-stained with 3E7 and antibodies to identify T-cells ($CD3^+$), T helper cells/monocytes ($CD4^+$), cytotoxic T-cells ($CD8^+$), and macrophages/monocytes ($ED1^+$). Flow cytometry data were analyzed by gating on $CD3^+$ cells (Fig. 3.17 A - C), $CD3^-$ cells (Fig. 3.17 D - F), $CD4^+$ cells (Fig. 3.17 G - I), $CD8^+$ cells (Fig. 3.17 J - L), and $ED1^+$ cells (data not shown). Specificity of double-staining was verified by using isotype control mouse IgG (Fig. 3.17 B, E, H, and K) and

non-specific fluorescence was subtracted from specific stains. Inflamed popliteal LN harbored 13 ± 4% $3E7^+$ T cells. An example is given in Fig. 3.17 C. $ED1^+3E7^+$ cells were below detection limit (data not shown). About 12 ± 3% of non-T-cells were $3E7^+$, an example is given in Fig. 3.17 F. 7 ± 4% of T helper cells/monocytes were $3E7^+$, as shown in Fig. 3.17 I. Gating on $CD8^+$ LN cells showed that 8 ± 3% were $3E7^+$. Fig. 3.17 L gives an example of $CD8^+3E7^+$ cells.

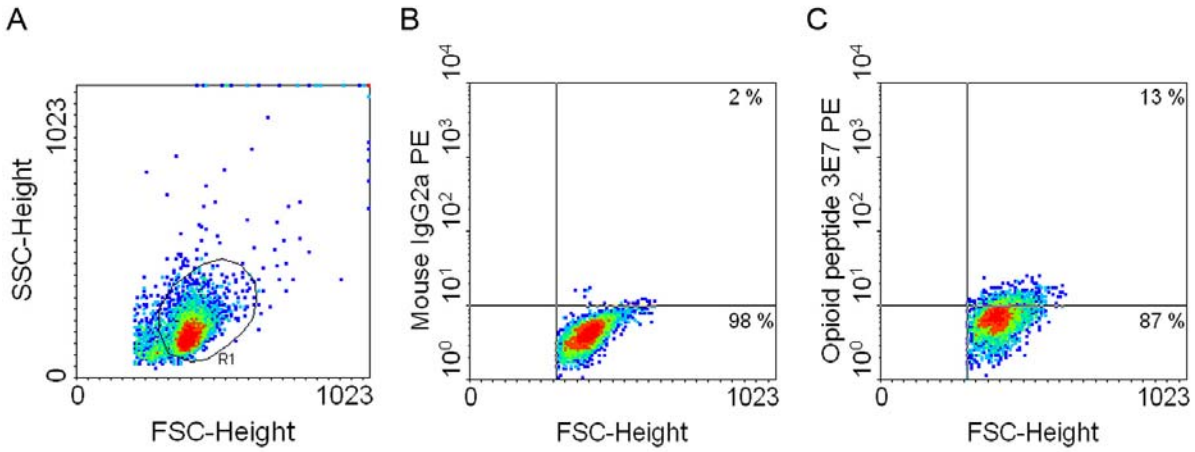

Fig. 3.16 Magnitude of opioid peptide-expression in inflamed LN cells. LN cells (96 h CFA) were stained with pan opioid antibody (3E7) or isotype matched control IgG and analyzed using flow cytometry. **A.** Gating. Density blot shows forward (FSC-Height, x-axis) vs. sideward scatter (SSC-Height, y-axis). **B + C.** Density blots show FSC-Height (x-axis) vs. log10 fluorescence (y-axis). **B.** Isotype control. **C.** $3E7^+$ LN cells of an animal with paw inflammation (96 h). Numbers of positive cells are given as percentages.

Fig. 3.17 (next page) Allocation of opioid peptide expression in LN cell subsets. LN cells (96 h CFA) were stained for opioid peptides using the antibody 3E7 or for its isotype. T-cells ($CD3^+$, panels **A - C**), non-T-cells ($CD3^-$, panels **D –F**), T helper cells and monocytes ($CD4^+$, panels **G - I**), and cytotoxic T-cells ($CD8^+$, panels **J - L**) were analyzed. **A.** $CD3^+$ gating. Density blot shows log10 fluorescence (x-axis) vs. SSC-Height (y-axis). **B + C.** Both axis show log10 fluorescence. **B.** Isotype control. **C.** $CD3^+3E7^+$ of an inflamed LN. **D.** $CD3^-$ gating. Density blot shows log10 fluorescence (x-axis) vs. SSC-Height (y-axis). **E + F.** Both axis show log10 fluorescence. **E.** Isotype control. **F.** $CD3^-3E7^+$ of an inflamed LN. **G.** $CD4^+$ gating. Density blot shows log10 fluorescence (x-axis) vs. SSC-Height (y-axis). **H + I.** Both axis show log10 fluorescence. **H.** Isotype control. **I.** $CD4^+3E7^+$ of an inflamed LN. **J.** $CD8^+$ gating. Density blot shows log10 fluorescence (x-axis) vs. SSC-Height (y-axis). **K + L.** Both axis show log10 fluorescence. **K.** Isotype control. **L.** $CD8^+3E7^+$ of an inflamed LN. Numbers of cells expressing 3E7 and/or surface markers are given as percentages in the quadrants.

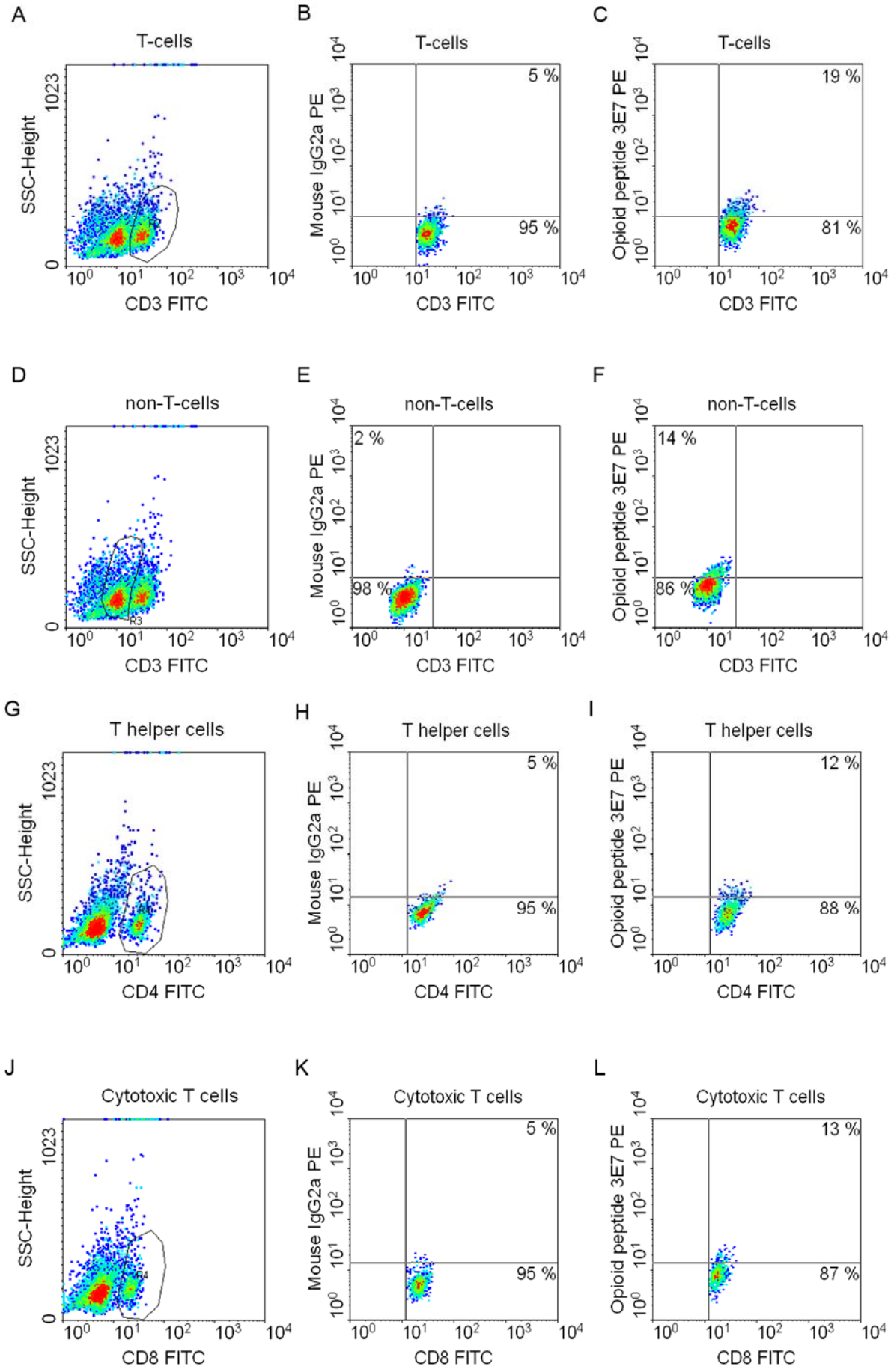
A
T-cells
SSC-Height
1023
0
CD3 FITC
B
T-cells
Mouse IgG2a PE
5 %
95 %
CD3 FITC
C
T-cells
Opioid peptide 3E7 PE
19 %
81 %
CD3 FITC
D
non-T-cells
SSC-Height
R3
CD3 FITC
E
non-T-cells
Mouse IgG2a PE
2 %
98 %
CD3 FITC
F
non-T-cells
Opioid peptide 3E7 PE
14 %
86 %
CD3 FITC
G
T helper cells
SSC-Height
CD4 FITC
H
T helper cells
Mouse IgG2a PE
5 %
95 %
CD4 FITC
I
T helper cells
Opioid peptide 3E7 PE
12 %
88 %
CD4 FITC
J
Cytotoxic T cells
SSC-Height
R4
CD8 FITC
K
Cytotoxic T cells
Mouse IgG2a PE
5 %
95 %
CD8 FITC
L
Cytotoxic T cells
Opioid peptide 3E7 PE
13 %
87 %
CD8 FITC

3.5 Quantification of END in lymphocytes

3.5.1 Increased ir-END levels in regional LN cells during inflammation

To test the hypothesis, that the production of END in leukocytes is increased by CFA-induced hindpaw inflammation, the END contents of peripheral blood leukocytes and draining LN cells were compared between controls and CFA-treated animals by RIA. In comparison to controls, cellular ir-END levels of peripheral blood leukocytes were significantly increased at 24 h after CFA-treatment (One-Way ANOVA, $P < 0.05$; Dunnett's Multiple Comparison Test, $P < 0.05$, Fig. 3.18 A). Ir-END levels in inflamed LN cells were significantly elevated at 12, 24, and 48 h after CFA-inoculation (One-Way ANOVA, $P < 0.0001$; Dunnett's Multiple Comparison Test: 0 vs. 12 h, $P < 0.01$; 0 vs. 24 h, $P < 0.01$; 0 vs. 48 h, $P < 0.01$; 0 vs. 96 h, $P > 0.05$; Fig. 3.18 B). Similar results were obtained in two other experiments analyzing the ir-END in LN cells but baseline values were different from that shown here (data not shown). To investigate whether the CFA-treatment produces a general upregulation of ir-END in secondary lymphoid tissues, ipsilateral inguinal LN cells were analyzed (Fig. 3.18 C). Ir-END levels of these inguinal lymphocytes showed no differences between controls and CFA-treated groups (One-Way ANOVA, $P > 0.05$, Fig. 3.18 C). Ir-END levels were then compared in popliteal and inguinal LN cells from the CFA-treated (ipsilateral) and untreated (contralateral) limbs (Fig. 3.18 D). The amount of ir-END per cell varied significantly between the different LN tissues analyzed (One-Way ANOVA, $P < 0.0001$). Both ipsi- and contralateral popliteal, but not ipsilateral inguinal LN cells showed significantly increased ir-END contents at 24 h after CFA in comparison to controls (Dunnett's Multiple Comparison Test: $LN_{pop\ ipsi}$ 0h vs $LN_{pop\ ipsi}$ 24h, $P < 0.01$; $LN_{pop\ ipsi}$ 0h vs $LN_{pop\ contra}$ 24h, $P < 0.01$; $LN_{pop\ ipsi}$ 0h vs $LN_{ing\ ipsi}$ 24h, $P > 0.05$; Fig. 3.18 D).

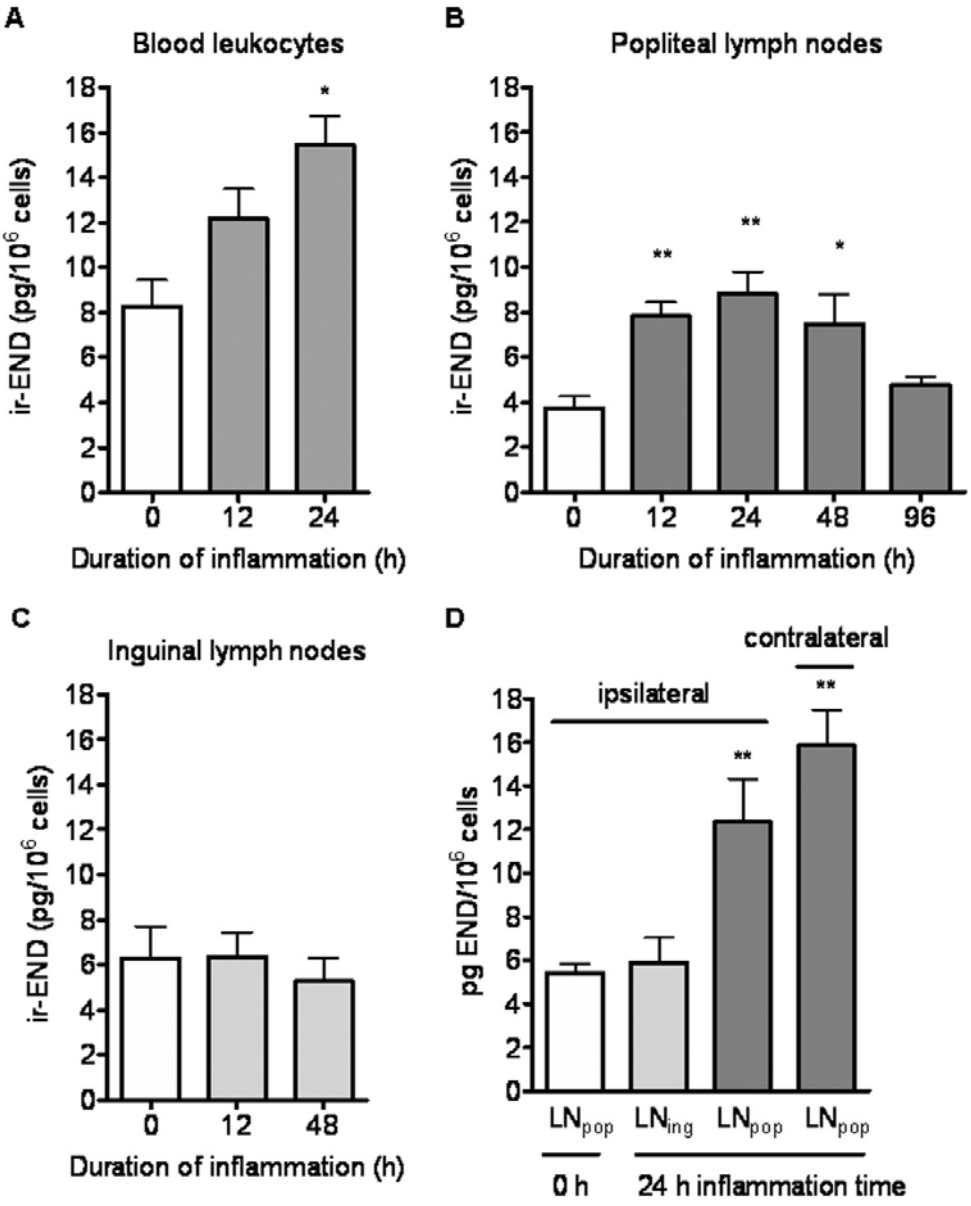

Fig. 3.18 Ir-END content in circulating leukocytes and in LN cells during inflammation. Ir-END was measured in immune cell lysates in duplicates using RIA. **A.** Ir-END in blood leukocytes at 0 - 24 h after CFA-treatment. Data represent the means ± SD of three animals per treatment group. **B.** Ir-END in popliteal LN cells at 0 - 96 h after CFA-treatment. For each sample cells from 3-15 animals were pooled. Data represent means ± SD of 3 - 4 samples per treatment group. **C.** Ir-END in inguinal LN cells at 0 - 48 h after CFA-treatment. Data represent means ± SD of 5 - 7 animals per treatment group. **D.** Ir-END in ipsilteral vs. contralateral LN cells at 0 - 24 h after CFA-treatment. For each sample cells from 5 - 10 animals were pooled. Data represent means ± SD of 3 - 4 samples per treatment group. Differences among CFA-treated and control groups were analyzed with One-Way ANOVA and Dunnett's Multiple Comparison Test; *P < 0.05; **P < 0.01.

3.5.2 $CD4^+$ T-cells show the highest increase of ir-END during inflammation

To analyze the cellular ir-END-content in subsets of LN cells draining normal and inflamed paw tissue, cell subsets were separated using magnetic beads to obtain $CD3^+$ and $CD3^-$ cells or $CD4^+$ T-cells and $CD4^-$ cells from total LN cell suspensions as described in the methods section. The purity of $CD3^+$ and $CD3^-$ cell fractions was as described above (see 'Expression of POMC mRNA in cell subsets of LN'). Magnetic separation of LN cells using anti-CD4 microbeads (after depletion of monocytes/macrophages with a FITC-labeled anti-ED1 and anti-FITC microbeads) revealed 90% pure CD4-positive and 80% pure CD4-negative fractions (data not shown). Ir-END levels in $CD3^+$ cells differed significantly between inflamed and control LN (One-Way ANOVA, $P < 0.05$). Increases were significant in inflamed LN at 24 h after CFA-injections (Dunnett's Multiple Comparison Test, $P < 0.05$, Fig. 3.19 A). Compared to $CD3^-$ cells from controls ir-END was significantly increased at 24 h after induction of inflammation (One-Way ANOVA, $P < 0.05$; Dunnett's Multiple Comparison Test, $P < 0.05$, Fig. 3.19 B). $CD4^+$ T-cells of inflamed LN contained significantly higher ir-END levels at 24 and 96 h than controls (One-Way ANOVA, $P < 0.05$; Dunnett's Multiple Comparison Test, $P < 0.05$, Fig. 3.19 C). Significantly higher ir-END levels in comparison to controls were detected at 24 and 48 h in macrophage/monocyte-depleted $CD4^-$ cells (One-Way ANOVA, $P < 0.05$; Dunnett's Multiple Comparison Test; $P < 0.01$, Fig. 3.19 D).

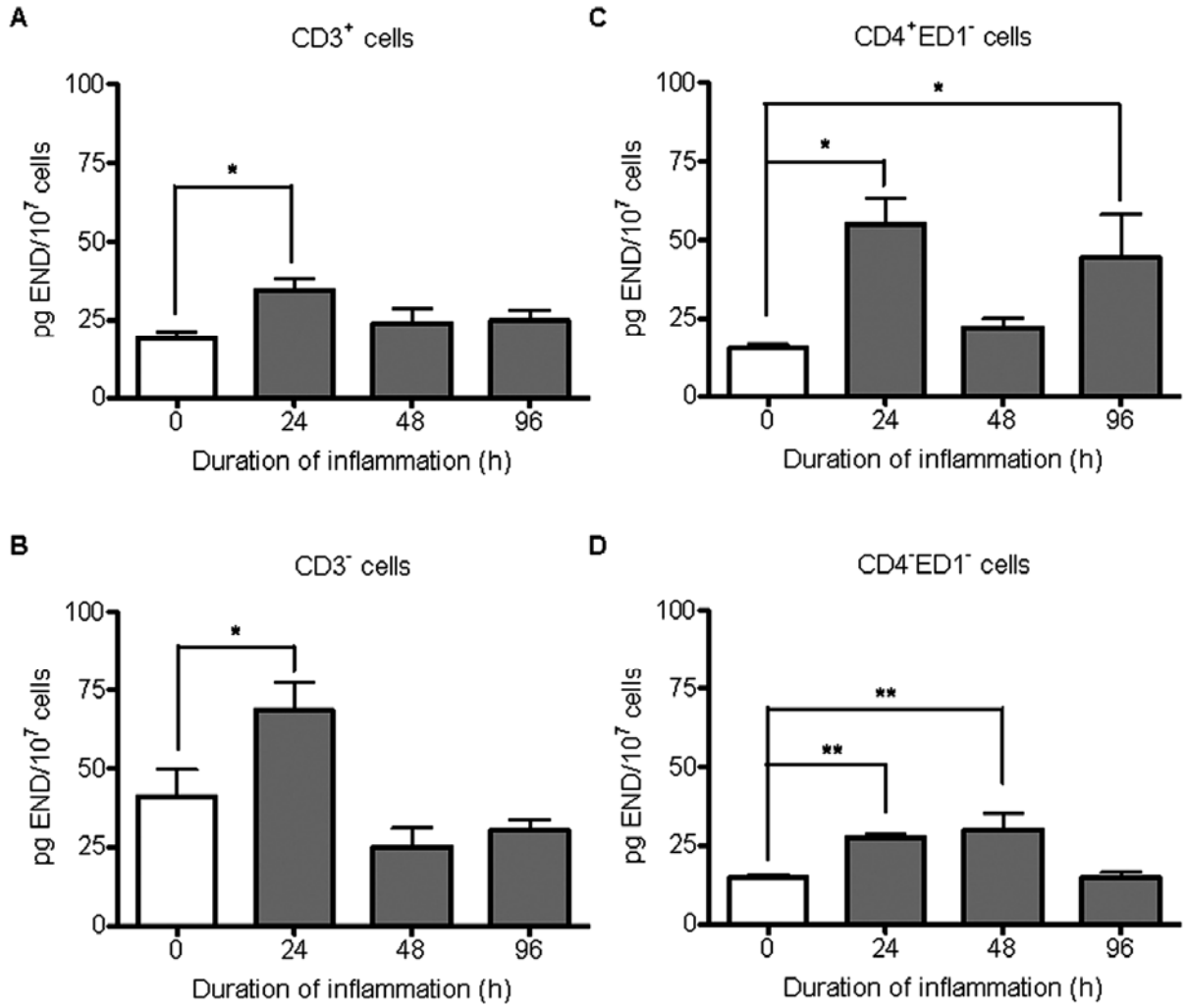

Fig. 3.19 Amount of ir-END in cell subsets of draining LN during inflammation. Ir-END was determined using RIA in lysed LN cell fractions after magnetic separation with anti-PanT (**A + B**) and anti-ED1/anti-CD4 (**C + D**) antibodies (0, 24, 48, and 96 h after CFA-treatment). Data represent means ± SD. **A.** Ir-END in $CD3^+$ cells. n = 4 - 5 animals per treatment group. **B.** Ir-END in $CD3^-$ cells. n = 6 animals per treatment group. **C.** Ir-END in $CD4^+$ $ED1^-$ cells. n = 4 animals per treatment group. **D.** Ir-END in $CD4^-$ $ED1^-$ LN cells. n = 4 animals per treatment group. Differences among CFA-treated and control groups were analyzed with One-Way ANOVA and Dunnett's Multiple Comparison Test; *P < 0.05; **P < 0.01.

3.6 IL-1β-induced POMC transcription and END synthesis in LN cells

To test the hypothesis, that cytokines such as interleukins are involved in the upregulation of lymphocytic POMC transcription during inflammation, relative POMC exon 2-3/rpL19 mRNA expression was analyzed after *ex vivo* stimulation of LN cells. Inflamed LN cells were stimulated for 24 h with 3, 10 and 30 ng per ml culture medium of IL-1α or IL-1β or with both agents. These pilot studies showed that relative POMC mRNA expression levels increased about 2-fold after stimulation with 3 and 10 ng IL-1β/ml while 30 ng IL-1β/ml showed no effect (data not shown). Relative POMC mRNA expression

levels were also increased after combined 24 h stimulation with 3 and 10 ng of each IL-1α and IL-1β whereas IL-1α alone showed no effect (data not shown). Based on these pilot experiments 5 ng IL-1β/ml was chosen for time course analysis. This IL-1β concentration lead to about 1.5-fold elevated POMC mRNA expression levels after 2, 4, and 12 h stimulation and to about 2-fold elevations at 24 h stimulation. Focusing on 2 h stimulation time the relative POMC mRNA expression was significantly upregulated over unstimulated controls (paired t test, $P < 0.05$, Fig. 3.20 A). The ir-END content was analyzed after 24 h stimulation of the cells with IL-1β. Ir-END was not increased in comparison to nonstimulated controls (paired t-test, $P > 0.05$, Fig. 3.20 B). Ir-END levels did also not increase during pilot experiments using 3, 10 and 30 ng of IL-1β/ml (data not shown). Testing was subsequently repeated with higher IL-1β doses from 10-1000 ng per ml culture medium. None of these doses induced an elevation of POMC gene transcription or ir-END levels within LN cells at 24 or 48 h (data not shown).

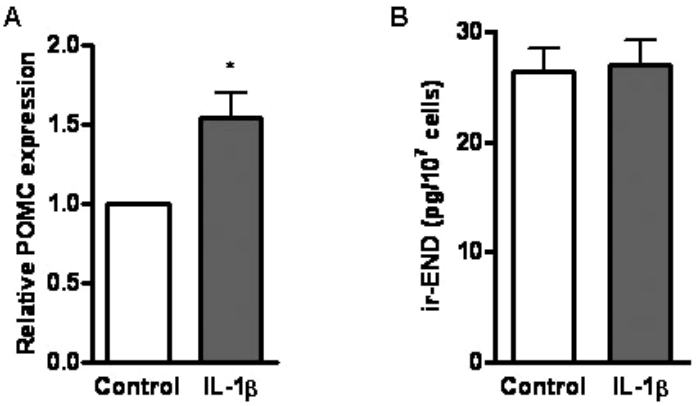

Fig. 3.20 Effect of IL-1β on the expression of POMC exon 2-3 mRNA and of ir-END in LN cells *in vitro*. LN cells were incubated with/without 5 ng IL-1β/ml culture medium. **A.** The relative POMC exon 2-3 mRNA expression was determined in 2 h IL-1β-stimulated vs. nonstimulated LN cells. Samples were measured in duplicate using semi-nested qRT-PCR. Values represent means ± SD of n = 6 animals. **B.** Ir-END was determined in the cell lysates after 24 h of stimulation. Data were analyzed with paired t test, *$P < 0.05$.